Population inversion and threshold current densities: A comparison of GaAs/(Al,Ga)As quantum-cascade structures with different barrier heights

L. Schrottke,[a] S. L. Lu, R. Hey, M. Giehler, H. Kostial, and H. T. Grahn
Paul-Drude-Institut für Festkörperelektronik, Hausvogteiplatz 5–7, 10117 Berlin, Germany

(Received 4 February 2005; accepted 18 April 2005; published online 16 June 2005)

The population of the laser levels in undoped GaAs/$Al_xGa_{1-x}As$ quantum-cascade structures (QCSs) is investigated by interband photoluminescence spectroscopy. We compare similar QCSs with different barrier heights ($x=0.33$ and $x=0.45$), for which the calculated population ratios ρ_p^{ca} are equal. While the experimental value ρ_p^{me} for $x=0.45$ agrees with the theoretical one, ρ_p^{me} for $x=0.33$ is much smaller than ρ_p^{ca}. At the same time, the threshold current densities j_{th} are significantly smaller for $x=0.45$ than for $x=0.33$. In the framework of a linear rate equation model, we estimate the effect of the experimentally observed reduction of the population ratio on j_{th}. We show that the increased value of j_{th} for $x=0.33$ cannot only be attributed to a larger leakage current due to the lower barriers, but also to the reduced population ratio. © *2005 American Institute of Physics*. [DOI: 10.1063/1.1929863]

I. INTRODUCTION

Quantum-cascade lasers (QCLs) based on GaAs/(Al,Ga)As heterostructures grown on GaAs are expected to play an important role for infrared lasers,[1–5] in particular, for longer wavelengths (terahertz radiation). Compared to (In,Ga)As/(In,Al)As QCLs grown on InP, however, the laser parameters, such as threshold current density j_{th} and temperature characteristics, are inferior for GaAs-based QCLs in the midinfrared spectral range. This difference is usually attributed to the lower conduction-band offset in the GaAs/(Al,Ga)As material system.

For most of the GaAs-based QCLs, (Al,Ga)As barriers with an Al content x of either 0.33 or 0.45 are used.[1,2] The larger effective barrier height for structures with $x=0.45$ is expected to reduce the leakage current into the quasicontinuum, which should result in both a reduction of j_{th} and an improvement of the temperature characteristics compared to structures with $x=0.33$. The poorer temperature performance for $x=0.33$ has been explained in terms of the degradation of the injection efficiency with temperature due to the thermally induced leakage current into the continuum levels.[2,6] In addition, Barbieri *et al.*[7] have carried out a systematic study of the influence of the injection barrier thickness on the leakage current from the injector to the continuum states for structures with $x=0.33$. They concluded that the leakage current can be suppressed for the thickest barrier at low temperatures, but is still present at higher temperatures due to thermal activation. Using an optimum design, room-temperature operation for GaAs-based QCLs can be achieved for $x=0.45$.[2]

The quantum-cascade structures (QCSs) reported by Sirtori *et al.*[1] for $x=0.33$ and Page *et al.*[2] for $x=0.45$ were designed in such a way that the calculated lifetimes and transition rates are very similar. The population ratio is defined as $\rho_p=n_{ul}/n_{ll}$ with n_{ul} and n_{ll} denoting the population of the upper and lower laser levels, respectively. As a first approximation, it is simply given by the ratio of the transition time from the upper to the lower laser level $\tau_{ul\to ll}$ and the total lifetime of the lower laser level τ_{ext}. The calculated ratio ρ_p^{ca} is 8 using the lifetimes $\tau_{ul\to ll}=2.4$ ps and $\tau_{ext}=0.3$ ps taken from Refs. 1 and 2. However, in a recent investigation of the coupling of the injector to the upper laser level by interband photoluminescence (PL) spectroscopy,[8] we have roughly estimated the population ratio ρ_p^{me} for $x=0.33$ to be only about 2. Furthermore, if the population ratios would actually be identical for both Al contents, the large difference of j_{th} could only be attributed to the (thermally activated) leakage current. Therefore, a detailed analysis of the laser level population and its correlation to the lasing properties of QCLs with different barrier heights would provide further insight into the effect of the leakage current on the threshold current density, which is critical for the improvement of the laser parameters.

II. THEORETICAL MODEL

Let us consider the correlation between ρ_p and j_{th} within the framework of linear rate equations for n_{ul} and n_{ll} including carrier injection I_{ul} into the upper laser level, transitions from the upper to the lower laser level with the respective relaxation time $\tau_{ul\to ll}$, escape from the upper laser level into other states such as, e.g., a direct transition into the ground state or into quasicontinuum states (τ_{esc}), recapture of carriers from states except the upper laser level into the lower laser level R_{ll}, and extraction from the lower laser level (τ_{ext})

$$\frac{dn_{ul}}{dt} = I_{ul} - \frac{n_{ul}}{\tau_{ul\to ll}} - \frac{n_{ul}}{\tau_{esc}}, \tag{1}$$

[a]Electronic mail: lutz@pdi-berlin.de

$$\frac{dn_{ll}}{dt} = R_{ll} + \frac{n_{ul}}{\tau_{ul\to ll}} - \frac{n_{ll}}{\tau_{ext}}. \tag{2}$$

For steady-state conditions, Eq. (1) results in

$$I_{ul} = n_{ul}\left[\frac{1}{\tau_{ul\to ll}} + \frac{1}{\tau_{esc}}\right] = \frac{n_{ul}}{\tau_{ul}} \tag{3}$$

and Eq. (2) in

$$\rho_p = \frac{n_{ul}}{n_{ll}} = \frac{\tau_{ul\to ll}}{\tau_{ext}} - R_{ll}\frac{\tau_{ul\to ll}}{n_{ll}}. \tag{4}$$

For $R_{ll}=0$, Eq. (4) leads to the common expression $\rho_p = \tau_{ul\to ll}/\tau_{ext}$. However, a nonvanishing R_{ll} would reduce the value of ρ_p. For the population difference, we obtain from the definition of ρ_p and Eq. (3)

$$\Delta n = n_{ul} - n_{ll} = \left(1 - \frac{1}{\rho_p}\right)n_{ul} = \frac{\rho_p - 1}{\rho_p} I_{ul}\tau_{ul}. \tag{5}$$

The population inversion ($\Delta n > 0$) can be decreased by a reduced population ratio and/or by an increased leakage current, i.e., a decreased value of τ_{ul}. Assuming that $j \propto I_{ul}$ and that the population inversion at lasing threshold Δn_{th} depends only on external parameters such as the resonator properties, i.e., $\Delta n_{th} = \text{const}$, we obtain

$$j_{th} \propto \frac{\Delta n_{th}}{\tau_{ul}}\frac{\rho_p}{\rho_p - 1} \propto \frac{1}{\tau_{ul}}\frac{\rho_p}{\rho_p - 1}. \tag{6}$$

This expression shows that j_{th} only increases by about 2% when ρ_p is decreased from 8 to 7. However, assuming $\rho_p \approx 2$ as estimated from interband PL spectra for a QCS with $x=0.33$,[8] j_{th} is expected to be already about 75% above the theoretical value, and any further reduction of ρ_p would lead to an additional increase of j_{th}. This effect may contribute to the large threshold current density in QCLs with $x=0.33$ in addition to the leakage current, which decreases the total lifetime τ_{ul} of the upper laser level.

III. EXPERIMENTAL DETAILS

The focus on GaAs-based systems enables us to compare QCLs with different barrier heights for almost identical wavelengths. At the same time, the PL experiments can be carried out for similar experimental conditions, since the band gap of the well material is the same (in both cases GaAs). For the determination of the population ratios, we use interband PL spectroscopy as described in Ref. 8. Because of the small value for ρ_p^{me} in the case of $x=0.33$, we investigate two samples with this Al content (A1 and A2), which were processed from two wafers grown with a nominally identical structure. Starting with the injection barrier, the layer sequence of one period is **5.8**, 1.5, **2.0**, 4.9, **1.7**, 4.0, **3.4**, 3.2, **2.0**, 2.8, **2.3**, 2.3, **2.5**, 2.3, **2.5**, and 2.1 nm (bold numbers indicate barriers). Sample B contains barriers with an Al content of $x=0.45$. The layer sequence for this sample is **4.6**, 1.9, **1.1**, 5.4, **1.1**, 4.8, **2.8**, 3.4, **1.7**, 3.0, **1.8**, 2.8, **2.0**, 3.0, **2.6**, and 3.0 nm. For both Al contents, we have also grown, processed, and characterized a number of QCLs.

The samples were grown by molecular-beam epitaxy on GaAs(100) substrates. The samples used for the PL measurement (A1, A2, and B) consisted of 20 periods with undoped injectors. The cladding layers were replaced by 400-nm-thick n^+-GaAs contact layers. For the optical experiments, the samples were processed into mesa structures with Ohmic ring contacts allowing optical access from the top of the mesa. The diameter of the mesas was typically about 200 μm. The samples were mounted on a cold finger in a He-flow cryostat, and the temperature was adjusted to 5 K. For the PL measurement, the samples were excited using a Ti:sapphire laser at a wavelength of 810 nm (1.531 eV) so that electrons and holes are only excited in the contact regions. The excitation power density was adjusted to a minimum for which a reasonable signal-to-noise ratio can be obtained. For the samples A1, A2, and B, we used excitation powers of 1 mW, 10 mW, and 10 μW, respectively. The laser beam was focussed onto a spot with a diameter of about 100 μm. The spectra were recorded with a charge-coupled device detector using a 1-m double monochromator.

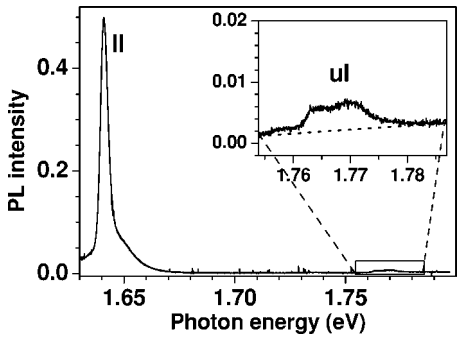

FIG. 1. PL spectrum of sample A1 ($x=0.33$) at 56 kV/cm. The inset depicts a magnification for the energy range of the upper laser level. The dotted line in the inset indicates the assumed background signal.

The corresponding lasers consist of 30 periods for $x=0.33$ and 36 periods for $x=0.45$ with doped injectors. While the sheet doping density per period was varied between 2.3×10^{11} and 1.0×10^{12} cm^{-2} for $x=0.33$ (see Ref. 9 for details), it was fixed at 3.9×10^{11} cm^{-2} for $x=0.45$. For this Al content, the typical dimensions of the laser stripes, which were prepared by plasma etching, are 19×3230 μm^2. The laser emission was studied using pulse-mode operation with a width of 100 ns and a repetition rate of 5 kHz. The infrared spectra were recorded using a Fourier-transform spectrometer. The spectra were measured at 7 K for a current density just above the threshold current density j_{th}.

IV. RESULTS AND DISCUSSION

Figures 1 and 2 show the normalized PL spectra of samples A1 and A2, respectively, for an electrical field strength of 56 kV/cm. The intensity ratio of the peak values for the upper and lower laser levels is $\rho_I = 0.004/0.5 = 0.008$ for sample A1 and $\rho_I = 0.01/0.44 = 0.023$ for sample A2. The peak values have been chosen instead of the integrated intensities since the laser is assumed to operate with an energy close to the gain maximum. With the calculated ratio for the transition matrix element at 56 kV/cm of $\rho_t = 0.006$, the experimental population ratio $\rho_p^{me} = \rho_I/\rho_t$ becomes 1.3 for A1 and 3.8 for A2. For the discussion below, we will use the average value of about 2.6. An increase of the excitation

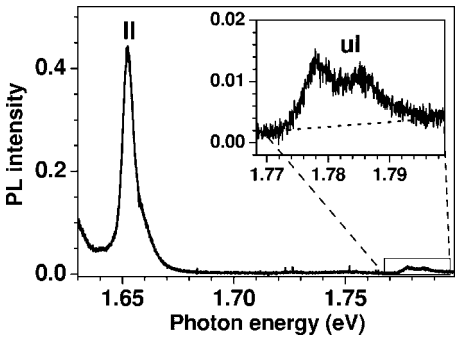

FIG. 2. PL spectrum of sample A2 ($x=0.33$) at 56 kV/cm. The inset depicts a magnification for the energy range of the upper laser level. The dotted line in the inset indicates the assumed background signal.

power by one order of magnitude shows an increase of the value for ρ_I by roughly 50%. For a smaller increase of the power, it merely fluctuates within about ±10%. The difference between the two samples may be in part attributed to the different excitation powers. Since an extrapolation to smaller power densities is not possible, we cannot exclude a certain overestimation of the value for ρ_p^{me} for samples A1 and A2. The material parameters used for this calculation are conduction-band offset $\Delta E_C=295$ meV (valence-band offset $\Delta E_V=159$ meV), effective electron mass $m_{e,w}^*=0.067m_0$ (effective heavy-hole mass $m_{\mathrm{hh},w}^*=0.377m_0$) for GaAs, and $m_{e,b}^*=0.08m_0$ ($m_{\mathrm{hh},b}^*=0.407m_0$) for $Al_{0.33}Ga_{0.67}As$, where m_0 denotes the free-electron mass. The nonparabolicity of the conduction band was taken into account by using a linear dependence of m_e^* on energy with a coefficient of $0.04m_0$ eV^{-1}, which was derived from an eight-band $\mathbf{k}\cdot\mathbf{p}$ model as, e.g., discussed in Ref. 10.

Both samples clearly show PL lines due to interband transitions between the upper (ul) as well as the lower (ll) laser level and the hole ground state. In addition, the upper laser level exhibits a splitting for both samples, which was already discussed in Ref. 8. This splitting is attributed to the coupling and anticrossing of the injector state with the upper laser level. The energy separation between the two subpeaks corresponds to the respective oscillation period found in femtosecond midinfrared pump-probe experiments.[11] The energy differences between the lower laser level and the two peaks in the energy range of the upper laser level are 126 (123) and 134 meV (129 meV) for sample A1 (sample A2). All these values are within the range of the lasing energies for respective QCLs, which lie between 115 and 135 meV.[9] For $x=0.33$, the average experimental value ρ_p^{me} is about $\rho_p^{\mathrm{ca}}/3$. Therefore, a reduced population ratio may be partially responsible for the higher threshold currents in GaAs-based QCLs with $x=0.33$.

The PL spectrum of sample B, which is shown in Fig. 3, contains several additional lines in comparison with samples A1 and A2, in particular, in the energy range of the lower laser level and the ground state. In order to identify the PL lines, we have calculated the interband transition energies and matrix elements for sample B using $\Delta E_C=393$ meV($\Delta E_V=212$ meV), $m_{e,b}^*=0.084m_0$($m_{\mathrm{hh},b}^*=0.417m_0$), and the energy gap for GaAs of 1.514 eV. The transitions of the upper laser

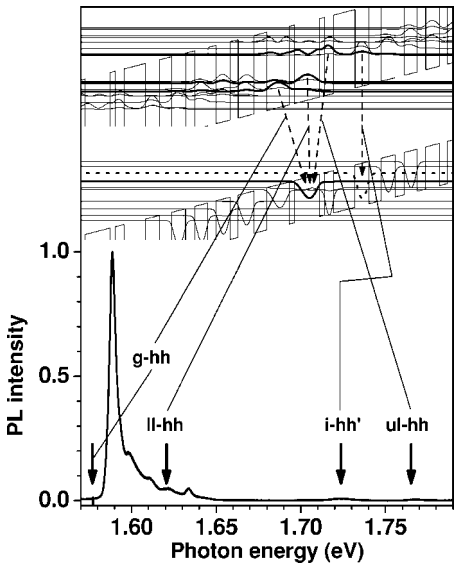

FIG. 3. PL spectrum of sample B ($x=0.45$) at 60 kV/cm. The top part shows a schematic view of the subband structure and the possible interband transitions.

level, the lower laser level, and the electron ground state with the hole ground state are marked by ul-hh, ll-hh, and g-hh, respectively, with the corresponding energies indicated by the arrows. While the measured transition energies for the upper and lower laser levels agree very well with the calculated values, the peak position of the ground state is shifted by about 10 meV. The peak at 1.723 eV can be attributed to the transition from the injector state to the hole ground state in the well in front of the injection barrier and is labeled i-hh′. The peaks at 1.598, 1.612, and 1.633 eV have not yet been identified. The peak at 1.633 eV exhibits a blueshift with increasing field, which is similar to the upper laser level, while the lower laser level and the ground state are redshifted. The blueshift indicates that the wave function has a nonvanishing part in the injector region rather than in the *extractor*, i.e., the injector of the following period. Therefore, this state cannot be related to the lower laser level.

Figure 4 shows a magnified part of the PL spectrum of sample B for the upper and lower laser levels. The energy difference between upper and lower laser levels of about 144

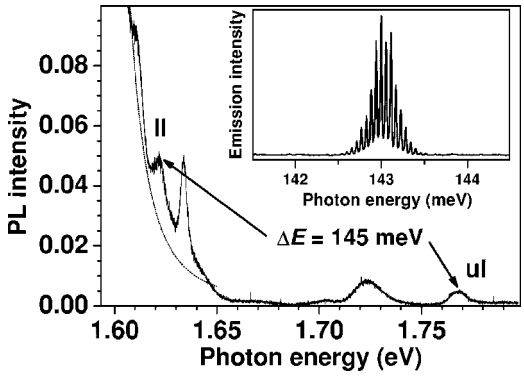

FIG. 4. Magnified part of the high-energy region of the PL spectrum shown in Fig. 3. The dotted line indicates a Lorentzian fit to the two peaks with the lowest energy used for the estimation of the background intensity. The inset presents a laser spectrum for one of the corresponding QCLs.

meV agrees very well with the lasing energies of respective QCLs, which vary between 142 and 147 meV. An example of a laser spectrum with an emission energy of 143 meV is shown in the inset of Fig. 4. In contrast with the PL spectra of samples A1 and A2, a splitting of the line attributed to the upper laser level is not detected for sample B, although a very similar oscillation period for the coherent electron transport has been reported for corresponding samples with $x=0.33$ and $x=0.45$.[11] All three QCSs exhibit a similar coupling, since the larger barrier height for $x=0.45$ is compensated by a smaller barrier width in sample B. In addition to the absence of any splitting of the upper laser level in sample B, a recent study of negative differential conductivity and current bistabilities has shown that QCSs with different Al content also differ with respect to their transport properties.[12] While for the $GaAs/Al_{0.45}Ga_{0.55}As$ QCS, the critical field strength, at which the bistable behavior occurs, is possibly smaller than the field strength, at which the upper laser level couples resonantly to the injector, both field strengths may coincide for the $GaAs/Al_{0.33}Ga_{0.67}As$ QCS.

The determination of ρ_p^{me} for sample B is more complicated than for samples A1 and A2, because the PL line due to the interband transition of the lower laser level is riding on the high-energy tail of the PL line of the ground-state transition. While the peak value for the upper laser level can be taken directly from Fig. 4, the determination of the peak value for the lower laser level requires the subtraction of a background signal, which we derive from a Lorentzian fit to the two PL peaks lowest in energy. For sample B, we estimate $\rho_I=0.005/0.02=0.25$ and obtain with $\rho_t=0.025$ an experimental population ratio of about 10, which is slightly above the theoretical value. An increase of the excitation power by up to two orders of magnitude does not show a significant change of the value for ρ_I. Note that the overlap between the upper laser level and the hole ground state is very small. At the same time, it actually depends on the electrical field strength so that the interband transition rate may be underestimated. Nevertheless, ρ_p^{me} for sample B is very close to the theoretical value, while the average value for samples A1 and A2 is clearly much smaller than ρ_p^{ca}. The splitting of the upper laser level in the $GaAs/Al_{0.33}Ga_{0.67}As$ QCSs may be in part responsible for the reduction of ρ_p.

Assuming $\rho_p=2.6$ for $x=0.33$, $\rho_p=10$ for $x=0.45$, and using Eq. (6), the injection current density for $x=0.33$ is estimated to be 1.46 times larger than the one for $x=0.45$ for a constant τ_{ul}. In comparison, for the set of QCLs with $x=0.33$ and medium doping concentration, the lowest measured value for j_{th} is 5.1 kA/cm^2, while it is 2.9 kA/cm^2 for QCLs with $x=0.45$, i.e., the value for $x=0.33$ is 1.76 times larger than the one for $x=0.45$. Therefore, we conclude that the larger j_{th} for $x=0.33$ may be attributed to both, a reduction of ρ_p and a larger leakage current due to the lower barriers, i.e., a smaller τ_{ul}. Note that we correlate the population properties measured in *undoped* QCSs with the threshold current densities in *doped* QCLs. Therefore, processes which depend on the carrier density, e.g., Auger processes, should have been taken into consideration. As a first approximation, however, we can assume that such processes modify the population properties in all samples in a similar way, since the QCLs for $x=0.33$ and $x=0.45$ have similar subband structures, lifetimes, and doping densities. A thorough discussion in how far carrier-density-dependent effects influence the population properties would require the study of the PL properties for operating lasers, which is rather difficult due to the high current levels. Although samples A1 and A2 are nominally identical, ρ_p^{me} for sample A2 is about three times larger than the one for sample A1. According to Eq. (4), the lower value of ρ_p for sample A1 may be caused by a larger recapture of carriers by the lower laser level from other states than the upper laser level (larger R_{ll}) or by a reduced extraction from the lower laser level (larger τ_{ext}).

V. CONCLUSIONS

In conclusion, we attribute the larger j_{th} for $GaAs/Al_{0.33}Ga_{0.67}As$ QCLs compared to lasers with $Al_{0.45}Ga_{0.55}As$ barriers only in part to an increased leakage current due to the lower barriers. Another significant contribution is caused by a reduced population ratio ρ_p. The reduction of ρ_p may be explained by the splitting of the upper laser level, which is only detected for $x=0.33$, and/or a recapture of electrons, which have escaped out of the upper laser level.

[1] C. Sirtori, P. Kruck, S. Barbieri, P. Collot, J. Nagle, M. Beck, J. Faist, and U. Oesterle, Appl. Phys. Lett. **73**, 3486 (1998).
[2] H. Page, C. Becker, A. Robertson, G. Glastre, V. Ortiz, and C. Sirtori, Appl. Phys. Lett. **78**, 3529 (2001).
[3] L. R. Wilson, P. T. Keightley, J. W. Cockburn, M. S. Skolnick, J. C. Clark, R. Grey, and G. Hill, Appl. Phys. Lett. **76**, 801 (2000).
[4] D. Indjin, S. Tomić, Z. Ikonić, P. Harrison, R. W. Kelsall, V. Milanović, and S. Kočinac, Appl. Phys. Lett. **81**, 2163 (2002).
[5] S. Anders, W. Schrenk, E. Gornik, and G. Strasser, Appl. Phys. Lett. **80**, 1864 (2002).
[6] P. Kruck, H. Page, C. Sirtori, S. Barbieri, M. Stellmacher, and J. Nagle, Appl. Phys. Lett. **76**, 3340 (2000).
[7] S. Barbieri, C. Sirtori, H. Page, M. Stellmacher, and J. Nagle, Appl. Phys. Lett. **78**, 282 (2001).
[8] L. Schrottke, R. Hey, and H. T. Grahn, Appl. Phys. Lett. **84**, 4535 (2004).
[9] M. Giehler, R. Hey, H. Kostial, S. Cronenberg, T. Ohtsuka, L. Schrottke, and H. T. Grahn, Appl. Phys. Lett. **82**, 671 (2003).
[10] P. Enders, A. Bärwolff, M. Woerner, and D. Suisky, Phys. Rev. B **51**, 16695 (1995).
[11] F. Eickemeyer, *et al.* Phys. Rev. Lett. **89**, 047402 (2002).
[12] S. L. Lu, L. Schrottke, R. Hey, H. Kostial, and H. T. Grahn, J. Appl. Phys. **97**, 024511 (2005).